

Dynamic light scattering in low connectivity phosphate glass melts crosslinked by Na or Zn

G. Dirks, J. Pereira and D. L. Sidebottom
Physics Department
Creighton University

Abstract

Dynamic light scattering was performed to measure the structural relaxation in sodium and zinc phosphate glass-forming melts in the range from 50 mol% to 40 mol% P_2O_5 where long polymer-like chains of PO_4 tetrahedra are systematically shortened in length. The findings reveal compositional changes in the non-exponentiality of the relaxation as well as in the glass fragility, the latter of which exhibits anomalous differences between sodium and zinc.

1. Introduction

Glass is a unique form of solidified matter[1,2]. It is most often formed when a liquid is cooled without the intervention of crystallization to become an amorphous solid. The metastable supercooled liquid that exists below the crystallization point, and which ultimately freezes into a solid, exhibits a host of complex dynamics[3-6] as its viscosity increases with increased cooling. This increased viscosity causes a dramatic slowing of molecular motions with typical reorientation times approaching 100s of seconds near the glass transition temperature, T_g . These are many orders slower than the nanosecond timescales[3] found in normal liquids above the melting point. Moreover, the molecular reorientations near the transition become highly cooperative in nature[4,5] requiring the concerted motion of neighboring molecules and this results in more complex relaxation processes that are both non-exponential and non-Arrhenius[7].

In the metastable state, the liquid will undergo structural relaxation that slows alongside the increasing viscosity. This is an equilibrium relaxation associated with the decay of spontaneous density fluctuations, $\delta\rho_q(t')$, occurring within the liquid that is captured by the dynamic structure factor[8,9],

$$S(q, t) = \frac{\langle \delta\rho_q(t) \delta\rho_q(t'+t) \rangle}{\langle \delta\rho_q(t') \rangle^2}, \quad (1)$$

where the inverse of the scattering wavevector, q^{-1} , sets a spatial scale for the size of the density fluctuations being probed. The dynamic structure factor is often monitored (in the frequency domain) by inelastic neutron scattering (with $q^{-1} \sim 1\text{\AA}$) but can also be monitored in the so-called hydrodynamic[10], $q^{-1} \sim \infty$, limit by light scattering at visible wavelengths. The decay of the dynamic structure factor is most often described by a Kohlrausch-Williams-Watts (KWW) or stretched exponential[3] of the form

$$S(q, t) \sim \exp\{-(t/\tau)^\beta\}, \quad (2)$$

where the exponent β is a fraction between zero and unity. Although the relaxation exhibits q -dependence for q near the first peak of the static structure factor[11], the relaxation becomes q -independent at smaller q as the hydrodynamic limit is approached[10]. The relaxation time, τ , is a measure of molecular motions that largely parallels the increase in liquid viscosity. However, the increase in relaxation time and viscosity with decreasing temperature rarely follow the sort of Arrhenius law ($\tau \sim \exp\{E/kT\}$) typical for simple dynamics involving thermally-activated transitions over energy barriers of size E . Instead, the relaxation time shows strong curvature when plotted in the Arrhenius fashion as a semi-log graph with inverse temperature as the abscissa. Indeed, the degree of curvature - a measure of the deviation from an Arrhenius law - varies considerably among glass-forming materials[1-3]. Materials with weak, isotropic van der Waals interactions that generally display the greatest non-Arrhenius behavior are often referred[3] to as "fragile" glass-formers, while network-forming oxides with strong, directional covalent bonds that most nearly conform to an Arrhenius law are classified as "strong". The fragility index, defined by the slope of the Arrhenius plot when the abscissa is scaled to the glass transition temperature,

$$m = \left. \frac{d \log_{10} \tau}{d(T_g/T)} \right|_{T \rightarrow T_g}, \quad (3)$$

is commonly employed to quantify the degree of non-Arrhenius behavior.

It is worth mentioning as an aside that, although the liquid is arrested at temperatures below T_g , the bulk solid that forms is still teeming with all sorts of localized dynamics[12]. These include not only vibrational motions, but also localized relaxations of the glass structure

and the diffusion of mobile ions which undergo activated hopping between charge-compensating sites to produce a measurable conductivity[13,14]. These ion-conducting solids feature prominently in recent efforts to design less hazardous ion battery materials and, here too, one finds evidence of complex dynamics in the form of a frequency-dependent conductivity caused by ionic relaxation that is generally non-exponential[15,16].

Many investigations of the structural relaxation in supercooled liquids have been conducted through the years using both light scattering[17,18] and dielectric spectroscopy[6]. By and large many of these studies have focused on simple molecular liquids (e.g., ortho-terphenyl) and polymers for which the glass transition resides below ambient temperatures. These materials with weak van der Waals interactions display a wide range of fragilities and non-exponentiality that are only loosely correlated[6,7]. By comparison, far fewer studies[19-22] have been carried out on network-forming oxides (NFOs) for which T_g is typically far above room temperature. This data gap is particularly unfortunate since these latter materials have the potential to offer valuable insight into the connections between glass structure and liquid dynamics. In the NFOs, well-documented systematic changes in the network structure[23,24] can be obtained merely by chemical substitutions. A classic example is the addition of alkali oxides to SiO_2 which generates non-bridging oxygens that serve to depolymerize the silicate network, decreasing the glass transition temperature and increasing the fragility[24].

In recent work, our group has been endeavoring to use dynamic light scattering - specifically, photon correlation spectroscopy - to study the dynamic structure factor in a variety of network-forming oxides including phosphate[20,21] and borate[19,22] glasses. Our goal is to understand how variations in network structure influence both the non-exponentiality and non-Arrhenius properties of the relaxation. Here, we report a study of sodium and zinc phosphate glasses with 50 to 60 mol% Na_2O or ZnO that extend from the metaphosphate into the polyphosphate range. Much like the alkali silicates described above, addition of modifiers to P_2O_5 generate the formation of non-bridging oxygens that depolymerize the network[25]. Owing to a double bonded oxygen, P_2O_5 itself forms a network of PO_4 tetrahedra each with just $n = 3$ bridging oxygen bonds. Addition of a modifier like Na_2O depolymerizes this network until at $x = 50$ mol% Na_2O , the structure consists of long polymer-like chains of PO_4 tetrahedra

each with just $n = 2$ bridging bonds. As one continues adding modifier, these chains become shortened due to the production of PO_4 tetrahedra with just $n = 1$ bridging oxygen that terminate the ends of the chain. In the model popularized by van Wazer[25], the chain length decreases as

$$N_{AVG} = \frac{2(100-x)}{(2x-100)}. \quad (4)$$

At the pyrophosphate composition, $x = 67\%$, this predicts chains reduced to a collection of PO_4 dimers interspersed with modifier ions and the shortening predicted by Eq. (4) is largely confirmed by experiment[25,26]

2. Experimental

2.1. Sample Preparation

Samples of $(\text{Na}_2\text{O})_x(\text{P}_2\text{O}_5)_{100-x}$ in the range from $x = 50$ to 56 were obtained by mixing appropriate amounts of two crystalline stocks ($x = 50$ and 60, respectively). Each of the two stocks was obtained by reacting ammonium dihydrogen phosphate, $\text{NH}_4\text{H}_2\text{PO}_4$, with Na_2CO_3 that had been filtered at 0.22 micron and recrystallized. The reaction was carried out at 500 C in a large porcelain dish and judged to be complete based on mass analysis. The resulting crystalline material was finely ground using a mortar and pestle and stored under dessicant. Similarly, samples of $(\text{ZnO})_x(\text{P}_2\text{O}_5)_{100-x}$ in the range from $x = 50$ to 60 were obtained from two glass stocks ($x = 50$ and 60, respectively). Each of the two stocks was obtained by reacting $\text{NH}_4\text{H}_2\text{PO}_4$ and ZnO in a silica crucible at 500 C and then fusing the melt near 900 C. The melt was splat quenched in small disks that were later finely ground.

In both series, a small amount (approx. 3 grams) of batch was loaded into a pre-cleaned silica ampoule (6 mm ID x 8 mm OD) that also served as the light scattering cell. The contents of the ampoule were then melted at 900 C to produce a transparent and colorless liquid that was degassed before taking light scattering measurements.

2.2. Photon Correlation Spectroscopy

Laser light (532 nm) from a stable laser (Coherent, Verdi 5) was focused into the ampoule by a $f = 50$ mm lens to produce a scattering volume with approximately 50 micron

beam waist. Light scattered from this volume was imaged by a second lens onto a 50 micron pinhole that was positioned approximately one-half meter in front of the photoactive region of a photomultiplier tube (EMI 9863B/350) operated in a single photon counting mode.

Photopulses from the photomultiplier tube were discriminated and digitized before being input to a commercial autocorrelator (Flex02-12D/C by correlator.com) that computed the intensity-intensity autocorrelation function, which under conditions of homodyne detection, is related to the dynamic structure factor as:

$$C(t) = \frac{\langle I(t)I(t+t) \rangle}{\langle I(t) \rangle^2} = 1 + A_{COH} |S(q, t)|^2. \quad (5)$$

For glassy materials the dynamic structure factor is dominated by the primary viscous (structural) relaxation for which

$$C(t) = 1 + A_{COH} |A \exp[-(t/\tau)^\beta]|^2. \quad (6)$$

The ampoule was maintained at a fixed temperature (± 0.2 C) using a homebuilt optical oven and measurements of the autocorrelation function were obtained at several selected fixed temperatures above the glass transition for each composition. The resulting autocorrelation functions were fit to the stretched exponential (Eqn. (6)) and the weighted average relaxation time was obtained as $\langle \tau \rangle = \frac{\Gamma(1/\beta)}{\beta} \tau$.

3. Results

Figure 1 shows the intensity autocorrelation functions from Na and Zn metaphosphate melts at a selection of temperatures and is typical of the correlation spectra we obtain. In all cases, the autocorrelation functions shift to longer times as temperature is lowered approaching hundreds of seconds near the glass transition point. While the scattering intensity of Zn phosphate melts was generally better than that from the sodium phosphate melts, reliable autocorrelations could be obtained in both cases and fit to Eqn. (6) to obtain the relaxation time and stretching exponent. Attempts to study sodium phosphate melts at $x > 56$ mol % were unsuccessful due to the appearance of strong scattering caused either by phase separation or the incipient nucleation of small crystalline particles in the melt.

From this, the average relaxation time could be determined for each composition over a large range of temperatures and plotted in the fashion of an Arrhenius law as shown in Fig. 2 for the instance of Zn metaphosphate. Although there is often some deviation from a straight line in this representation, a substantial range of several decades form a nearly straight line at long relaxation times allowing an extrapolation to 100 seconds where the glass transition temperature is then determined. Values of the transition temperature are shown in Fig. 3 and are seen to be consistent with values reported in the literature[26,27]. Once this transition temperature is known, a plot of Fig. 2 is re-generated with the temperature scaled to the glass transition temperature to produce what some might refer to as an "Angell plot"[3] wherein the slope near T_g is a direct measure of the fragility index (see inset to Fig. 2).

As shown in Fig. 4, the fragility of the two glass series display remarkably different compositional trends as the phosphate chains are being shortened. In the Zn series, the fragility of the metaphosphate is quite low near $m = 30$ and increases only slightly to $m = 40$ at $x = 60$ mol% ZnO. However, in the Na series the fragility of the metaphosphate is large at $m = 90$ and decreases rapidly with depolymerization. In the figure, values of the fragility obtained from calorimetry[28] have been included for comparison and an additional horizontal scale has been added to indicate the approximate average length of a phosphate chain as predicted by van Wazer's theory (see Eqn. (4)).

Values of the stretching exponent are plotted as a function of the average relaxation time for both glass series in Fig. 5. This choice for the abscissa is necessitated by the large differences in fragility: plotted as a function of temperature the data for the Na series would be highly compressed in relation to that for the Zn series. In this manner, data for both series are better compared as their relaxation times slow on approach to 100 seconds at T_g . Although there is some scatter in the results, the scatter is largely in keeping with the typical error (about ± 0.05 and indicated in the figure by error bars for $x = 50$ mol%) in determining this parameter from an individual autocorrelation spectrum. Although there is no discernable trend in either series alone, the average stretching exponent for the Na case ($\beta = 0.38 \pm 0.05$) is decidedly smaller than that ($\beta = 0.58 \pm 0.05$) seen for the Zn series.

4. Discussion

As for the non-exponentiality of the relaxations, we observe little or no detectable dependence of the stretching parameter with either temperature or composition in either series. Nevertheless, the average value of this parameter overall is larger in the case of Zn than in Na and this is aligned with a general perception by many[6] that glasses with high fragility are apt to be more non-exponential. For the fragility, there are starkly different compositional trends between Zn and Na. In the instance of Zn, the fragility is low but increases slightly with depolymerization of the phosphate chains, while in the case of Na, the fragility is high but decreases with depolymerization. Our earlier studies of sodium ultraphosphates[21] had suggested a systematic dependence of the fragility index on the average bridging oxygen bond density, $\langle n \rangle$, wherein fragility generally increased as bridging oxygens were removed from the network structure. With $\langle n \rangle = 3$, P_2O_5 was found[20] to be an extremely strong glass-former with $m \approx 20$, but this fragility increased continuously as sodium was added culminating in a very fragile melt with $m \approx 80$ to 90 at the metaphosphate composition in which long PO_4 chains ($\langle n \rangle = 2$) are weakly crosslinked by the sodium ions.

This pattern was seen to identically mimic[21] that of the fragility of chalcogenide glasses[29] whose network connectivity was described by the average (atomic) bond density, $\langle r \rangle$. Here too, the fragility was near 80 at $\langle r \rangle = 2$ but decreased in an identical manner as $\langle r \rangle$ increased due to the addition of atomic-level crosslinking atoms (As with $r = 3$ and Ge with $r = 4$). In later work, this similarity led us to eventually propose a *coarse-grained model* (CGM) for the fragility in network-forming glasses[30-32]. This model proposes that the fragility of all network-forming glasses can be described by a single master curve as a function of a generalized connectivity, ϕ . In most cases, ϕ is identical with either $\langle r \rangle$ or $\langle n \rangle$. But in instances of larger rigid structural units (e.g., small rings), additional coarse-graining[30] is needed to identify redundant bridging oxygen connections and properly determine ϕ . Support for the model is evidenced by the collapse of the fragility from more than 150 different network-forming glasses onto a common curve[31] that decreases from $m \approx 90$ at $\phi = 2$ to $m \approx 20$ at $\phi \gtrsim 3$.

In a recent study of metaphosphates, Sen and coworkers[33] demonstrated that while modifying ions (like Na) with low field strength tend not to contribute to the network connectivity in the same sense that a P-O-P linkage would, ions with higher field strength (like Zn, Mg) do appear to form strong linkages that increase the network connectivity, ϕ . This distinction is supported by others[34] and provides a simple explanation for the low fragility of the Zn metaphosphate compared with that of the Na metaphosphate seen in Fig. 4. In fact, in our study of mixtures of Na and Zn metaphosphates[35], we applied the CGM to suggest that the connectivity of Zn metaphosphate is nearer to $\phi \approx 3$ (rather than 2) owing to the possible formation of Zn linkages with PO_4 tetrahedra that are either corner sharing or edge sharing in nature. Within the CGM approach, an edge-sharing linkage represents the appearance of a redundant bridging oxygen connection since the two bridging oxygens shared between PO_4 and ZnO_4 units function, topologically, as a single lattice connection. The presence of these redundant connections serves to lower the network connectivity, ϕ . For this reason, we could anticipate an increase of fragility for Zn polyphosphates like that seen in Fig. 4 to result from a decrease of connectivity as the phosphate chains themselves are being shortened. This shortening results in greater numbers of $n = 1$ phosphate units (which terminate chains at each end) and also introduce the possibility of face sharing connections with the Zn cation that introduce additional redundant bridging oxygen bonds that can further reduce the coarse-grained connectivity (and so increase fragility).

It is also worth noting that trends in both T_g and density of Zn phosphate glasses have been correlated with changes in the network structure particularly the coordination number of the Zn polyhedron[25,36]. In the compositions below 50 mol% ZnO, the Zn ions appear as isolated units corner sharing only with phosphate units. But as the concentration of Zn increases into the polyphosphate regime, Zn begins to cross link with other Zn to form a subnetwork[37] of ZnO wherein it is the fragments of phosphate chains that are now isolated. Although these structural changes do correlate with T_g it is unclear how they might influence the fragility. In our experience, changes in the fragility are often unrelated to changes in T_g [38]. Indeed, in a recent study[28] of Zn phosphates reporting both fragility and T_g it appears

that the minimum in T_g seen near 55 mol% Zn is not replicated in the fragility whose value is largely constant between 35 to 50 mol%.

The situation for the sodium series is far more challenging to interpret and appears to defy a general trend that fragility increases as covalent bonds are removed from a network. On the one hand, it is unclear whether the same notions of connectivity used to develop rigidity theory[39] and the CGM for network materials have application for systems with $\phi < 2$. As further depolymerization proceeds, the material must degrade into a "soup" of small oligomeric pieces with a growing density of so-called "dangling ends" (e.g., the $n = 1$ phosphate units). Although these units fail to connect via bridging oxygen bonds, it should be acknowledged that the coulombic bond strength between the $n = 1$ phosphate unit and the Na ion is stronger than that between the Na ion and a $n = 2$ phosphate unit[40] and this might account for some strengthening of the network in spite of the decreasing levels of connectivity.

On the other hand, the observation of decreasing fragility with depolymerization is not unprecedented and has been seen in some polymer melts. Sokolov[41] recently noted this anomalous fragility trend in certain polymers (e.g., polystyrene, PS) wherein the fragility index increases sharply with increasing molecular weight (MW), doubling from $m = 70$ to over 160 as the MW of PS increased from 197 to over 2×10^5 . Given a monomer molecular weight of 104 g/mol, this MW range would roughly correspond to melts with average chain lengths ranging from 2 to 2000 monomers, respectively. Oddly, other polymers, like poly(propylene oxide) and poly(dimethyl siloxane), display little or no dependence of the fragility on their molecular weight[41]. Although the reason for the differences remains tenuous, Sokolov has suggested the strong increase in fragility with MW in polystyrene may be a consequence of its more rigid backbone chemistry. Other polymers, like poly(dimethyl siloxane), have more flexible backbones allowing the structural relaxation to occur by local segmental motions which become decoupled over a very short distance. Because of this localized motion, these polymers fail to exhibit any dependence of fragility on molecular weight. By contrast, in polymers like PS that have a stiff backbone the structural relaxation is proposed to involve larger segments of the polymer chain. According to Sokolov[41], this results in increased frustration with increasing molecular weight that increases both the glass transition and the fragility.

5. Conclusion

Photon correlation spectroscopy reported here provides a rare look into the non-exponential and non-Arrhenius dynamics of covalently bonded network-forming melts in the vicinity of the glass transition. In many of these materials the fragility is closely related to the average bond density of the network - increasing with increasing depolymerization of the network as the bond density decreases toward that of a polymeric fluid with $\phi = 2$. The present investigation of melts intermediate between metaphosphate and pyrophosphate represents an exploration into systems for which the bond connectivity decreases below $\phi = 2$ - where PO_4 chains become shortened and the melt begins to transform into that of an ionic liquid; a mixture of Na or Zn ions along with $[\text{P}_2\text{O}_7]^{4-}$ anions in the pyrophosphate limit. Our results suggest that the dynamics depend sensitively on the nature of the ion: Zn phosphates become more fragile with shortening of the PO_4 chains while Na phosphates rapidly become less fragile. Although some of this difference may be attributed to the differing field strength of the two ions that permits Zn to form stronger crosslinking bonds with the PO_4 chains (while Na is ineffective in this regard), the decreasing fragility in the sodium phosphates remains an anomaly that will require further investigations.

Acknowledgement

This work was supported through NSF grant DMR-2051396. The assistance of Harsh Uppala in data collection and analysis is gratefully appreciated.

References

1. P.G. Debenedetti, F.H. Stillinger, Supercooled liquids and the glass transition, *Nature* 410 (2001) 259 - 267.
2. J.C. Dyre, Colloquium: The glass transition and elastic models of glass-forming liquids, *Rev. Mod. Phys.* 78 (2006) 953 - 972.
3. M.D. Ediger, C.A. Angell, S.R. Nagel, Supercooled liquids and glasses, *J. Phys. Chem.* 100 (1996) 13200-13212.

4. M.D. Ediger, Spatially Heterogeneous Dynamics in Supercooled Liquids, *Annu. Rev. Phys. Chem.* 51 (2000) 99 - 128.
5. M.D. Ediger, P. Harrowell, Perspective: Supercooled liquids and glasses, *J. Chem. Phys.* 137 (2012) 080901.
6. R. Boehmer, K.L. Ngai, C.A. Angell, D.J. Plazek, Nonexponential relaxations in strong and fragile glass formers, *J. Chem. Phys.* 99(5) (1993) 4201 - 4209.
7. J.C. Dyre, Ten themes of viscous liquid dynamics, *J. Phys. Condens. Matter* 19 (2007) 205105.
8. Berne, B. J. and Pecora, R. *Dynamic Light Scattering* (John Wiley & Sons, New York, 1976).
9. D.L. Sidebottom, Dynamic Light Scattering in *Characterization of Materials* ed. by Elton N. Kaufmann (John Wiley & Sons, 2012).
10. R.D. Mountain, Generalized hydrodynamics, *Advances in Molecular Relaxation Processes* 9 (1977) 225-291.
11. J. Colmenero, A. Arbe, A. Alegria, Crossover from Debye to non-Debye dynamical behavior of the α -relaxation observed by quasielastic neutron scattering in a glass-forming polymer, *Phys. Rev. Lett.* 71(16) (1993) 2603-2606.
12. K.L. Ngai, Dynamic and thermodynamic properties of glass-forming substances, *J. Non-Cryst. Solids* 275 (2000) 7-51.
13. H. Jain, W.C. Huang, E.I. Kamitsos, Y.D. Yiannopoulos, Significance of intermediate range structure for electrical conduction in alkali germanate glasses, *J. Non-Cryst. Solids* 222 (1997) 361-368.
14. C.A. Angell, Fast ion motion in glassy and amorphous materials, *Solid State Ionics* 9&10 (1983) 3-16.
15. H. Jain, S. Krishnaswami, Composition dependence of frequency power law of ionic conductivity of glasses, *Solid State Ionics* 105 (1998) 129-137.
16. D.L. Sidebottom, Colloquium: Understanding ion motion in disordered solids form impedance spectroscopy scaling, *Rev. Mod. Phys.* 81 (2009) 999-1014.
17. D.L. Sidebottom, C.M. Sorensen, Dynamic light scattering study of non-exponential relaxation in supercooled $2\text{Ca}(\text{NO}_3)_2\text{3KNO}_3$, *J. Chem. Phys.* 91 (1989) 7153 - 7158.

18. D.L. Sidebottom, C.M. Sorensen, A light-scattering study of the glass transition in salol, *Phys Rev. B* 40 (1989) 461 - 466.
19. D.L. Sidebottom, R. Bergman, L. Börjesson, L.M. Torell, Two-step relaxation decay in a strong glass-former, *Phys. Rev. Lett.* 71 (1993) 2260 - 2263.
20. D.L. Sidebottom, J.R. Changstrom, Viscoelastic relaxation in molten phosphorus pentoxide using photon correlation spectroscopy, *Phys. Rev. B* 77 (2008) 020201.
21. R. Fabian, Jr., D.L. Sidebottom, Dynamic light scattering in network-forming sodium ultraphosphate liquids near the glass transition, *Phys. Rev. B* 80 (2009) 064201.
22. H.G. Uppala, D.L. Sidebottom, Evidence for ionic diffusion in dynamic light scattering from glass-forming sodium borate melts *J. Non-Cryst. Solids* 588 (2022) 121627.
23. W.H. Zacharien, The atomic arrangement in glass, *J. Am. Chem. Soc.* 54 (1932) 3841-3851.
24. Zarzycki, J. *Glasses and the vitreous state*. Cambridge: University Press; 1991.
25. R.K. Brow, Review: the structure of simple phosphate glasses, *J. Non-Cryst. Solids* 263&264 (2000) 1-28.
26. B. Tischendorf, J.U. Otaigbe, J.W. Wiench, M. Pruski, B.C. Sales, A study of short and intermediate range order in zinc phosphate glasses, *J. Non-Cryst. Solids* 282 (2001) 147-158.
27. R.K. Brow, C.A. Click, T.M. Alam, Modifier coordination and phosphate glass networks, *J. Non-Cryst. Solids* 274 (2000) 9 - 16.
28. Y. Xia, H. Chen, I. Hung, Z. Gan, S. Sen, Structure and fragility of Zn-phosphate glasses: Results from multinuclear NMR spectroscopy and calorimetry, *J. non-Cryst. Solids* 580 (3033) 121398.
29. M. Tatsumisago, B.L. Halfpap, J.L. Green, S.M. Lindsay, C.A. Angell, Fragility of Ge-As-Se glass-forming liquids in relation to rigidity percolation and the Kauzmann paradox, *Phys. Rev. Lett.* 64 (1990) 1549-1552.
30. D.L. Sidebottom, S.E. Schnell, Role of intermediate-range order in predicting the fragility of network-forming liquids near the rigidity transition, *Phys. Rev. B* 87 (2013) 054202.
31. D.L. Sidebottom, Fragility of network-forming glasses: A universal dependence on the topological connectivity. *Phys. Rev. E* 92 (2015) 062804.

32. D.L. Sidebottom, Connecting glass-forming fragility with network topology, *Front. Mater.* 6 (2019) 144.

33. Y. Xia, W. Zhu, M. Lockhart, B. Aitken and S. Sen, Fragility and rheological behavior of metaphosphate liquids: Insights into their chain vs. network characters, *J. Non-Cryst. Solids* 514 (2019) 77-82.

34. B.P. Rodrigues, L. Wondraczek, Medium-range topological constraints in binary phosphate glasses, *J. Chem. Phys.* 138 (2013) 244507.

35. D.L. Sidebottom, D. Vu, Assessing the network connectivity of modifier ions in metaphosphate glass melts: A dynamic light scattering study of Na-Zn mixtures, *J. Chem. Phys.* 145 (2016) 164503.

36. U. Hoppe, A structural model for phosphate glasses, *J. Non-Cryst. Solids* 195 (1983) 138 – 147.

37. Y. Onodera, S. Kohara, H. Masai, A. Koreeda, S. Okamura, T. Ohkubo, Formation of metallic cation-oxygen network for anomalous thermal expansion coefficients in binary phosphate glass, *Nature Comm.* 8 (2017) 15449.

38. D. L. Sidebottom, Coarse-grained model of the glass transition in network-forming oxides, *J. Am. Ceram. Soc.* 104 (2021) 2007 – 2016.

39. M.F. Thorpe, Continuous deformations in random networks, *J. Non-Cryst. Solids* 57 (1983) 355 - 370.

40. R. J. Kirkpatrick, R. K. Brow, Nuclear magnetic resonance investigation of the structures of phosphate and phosphate-containing glasses: A review, *Solid State Nuclear Magnetic Resonance* 5 (1995) 9 -21.

41. A.P. Sokolov, V.N. Novikov, Y. Ding, Why many polymers are so fragile, *J. Phys.: Condens. Matter* 19 (2007) 205116.

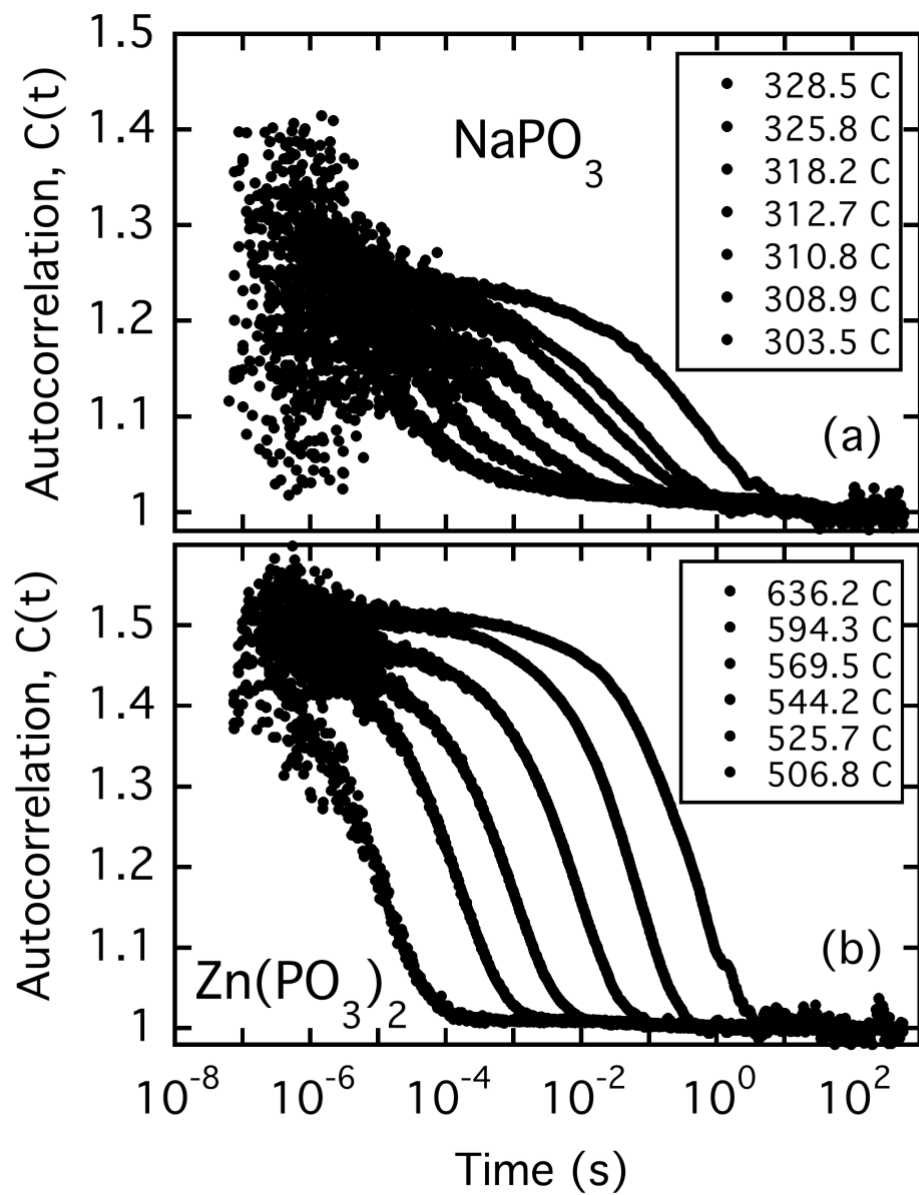


Fig. 1 Autocorrelation functions obtained for (a) sodium and (b) zinc metaphosphate melts at selected temperatures indicated in the key. Spectra advance to longer times with decreasing temperature.

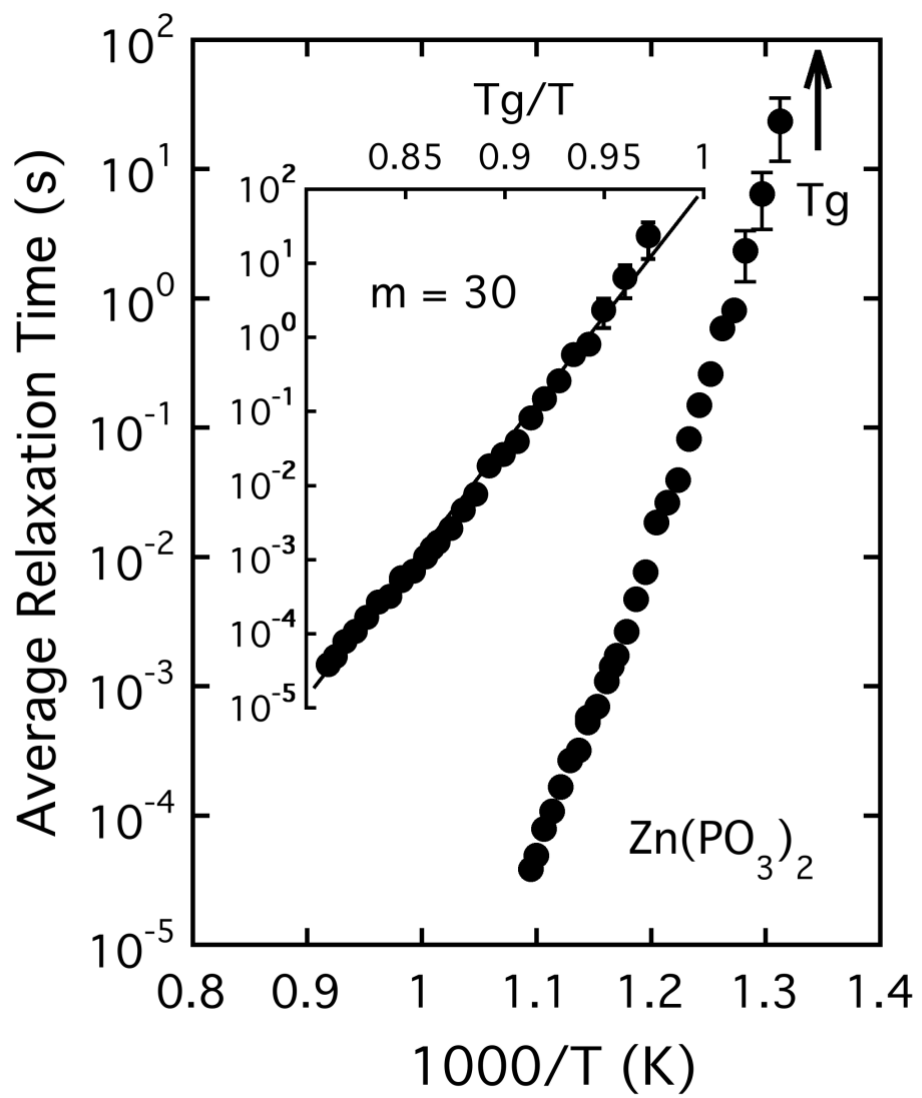


Fig. 2 The average relaxation time for zinc metaphosphate melt is plotted against inverse temperature to demonstrate the nearly Arrhenius trend extrapolated to determine the glass transition temperature. Inset shows the same only with the abscissa rescaled by the glass transition temperature so that the fragility index, $m = 30$ (± 2), can be assessed directly from the slope of the curve.

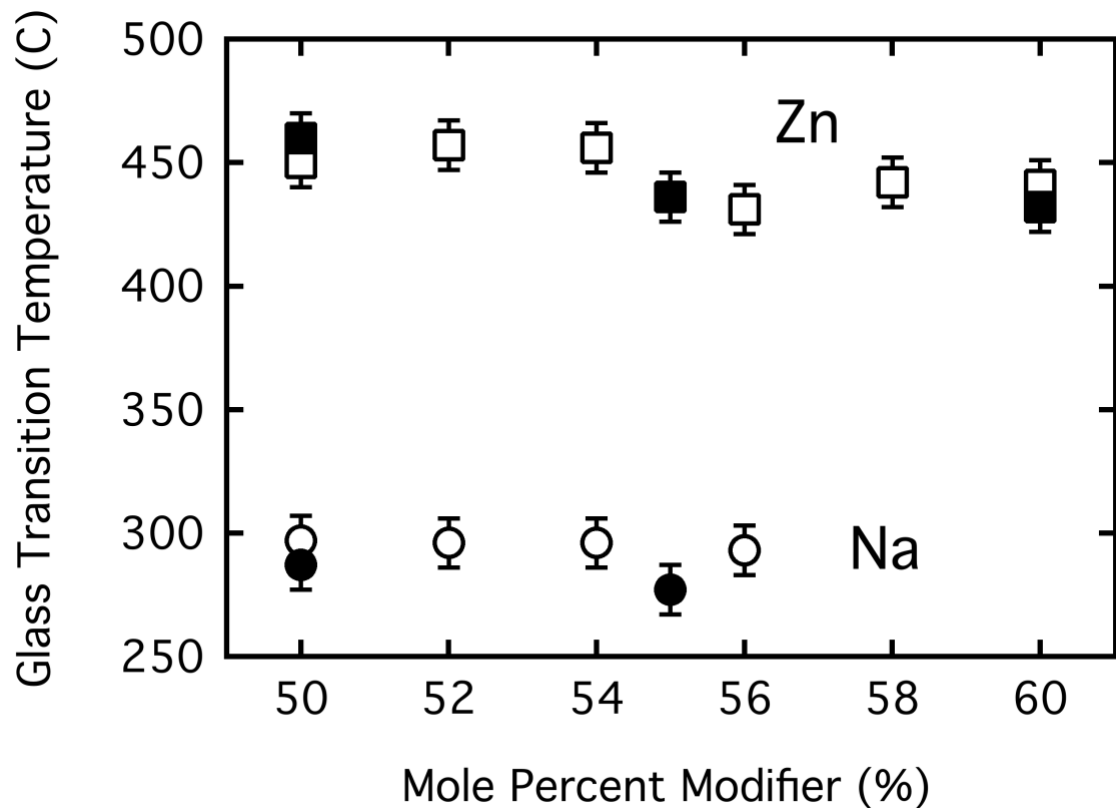


Fig. 3 The glass transition temperatures as obtained from analysis of the PCS dataset (open symbols) are compared with values from literature (solid squares[26], solid circles[27]).

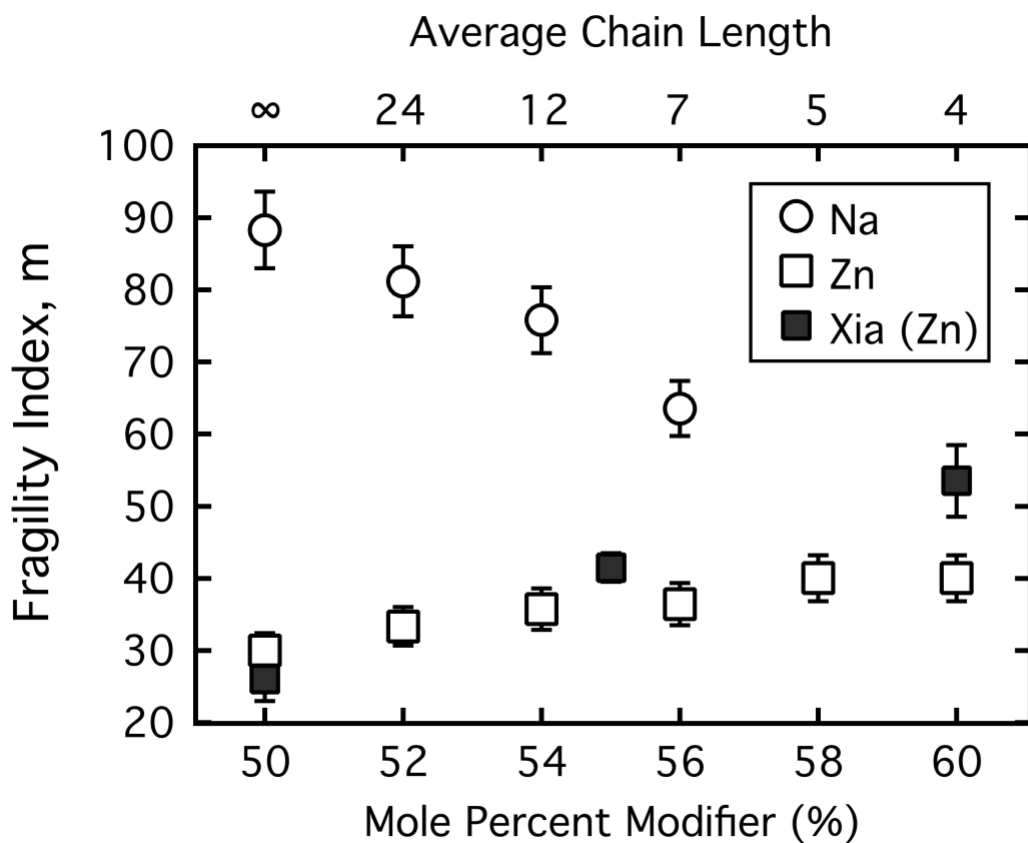


Fig. 4 The fragility of the sodium and zinc phosphate melts obtained from analysis of the PCS dataset (open symbols) display contradictory trends with increasing depolymerization of the phosphate chains. Fragility data obtained from calorimetry[28] are also included for comparison. Chain length displayed on upper abscissa was determined from Eqn. (4).

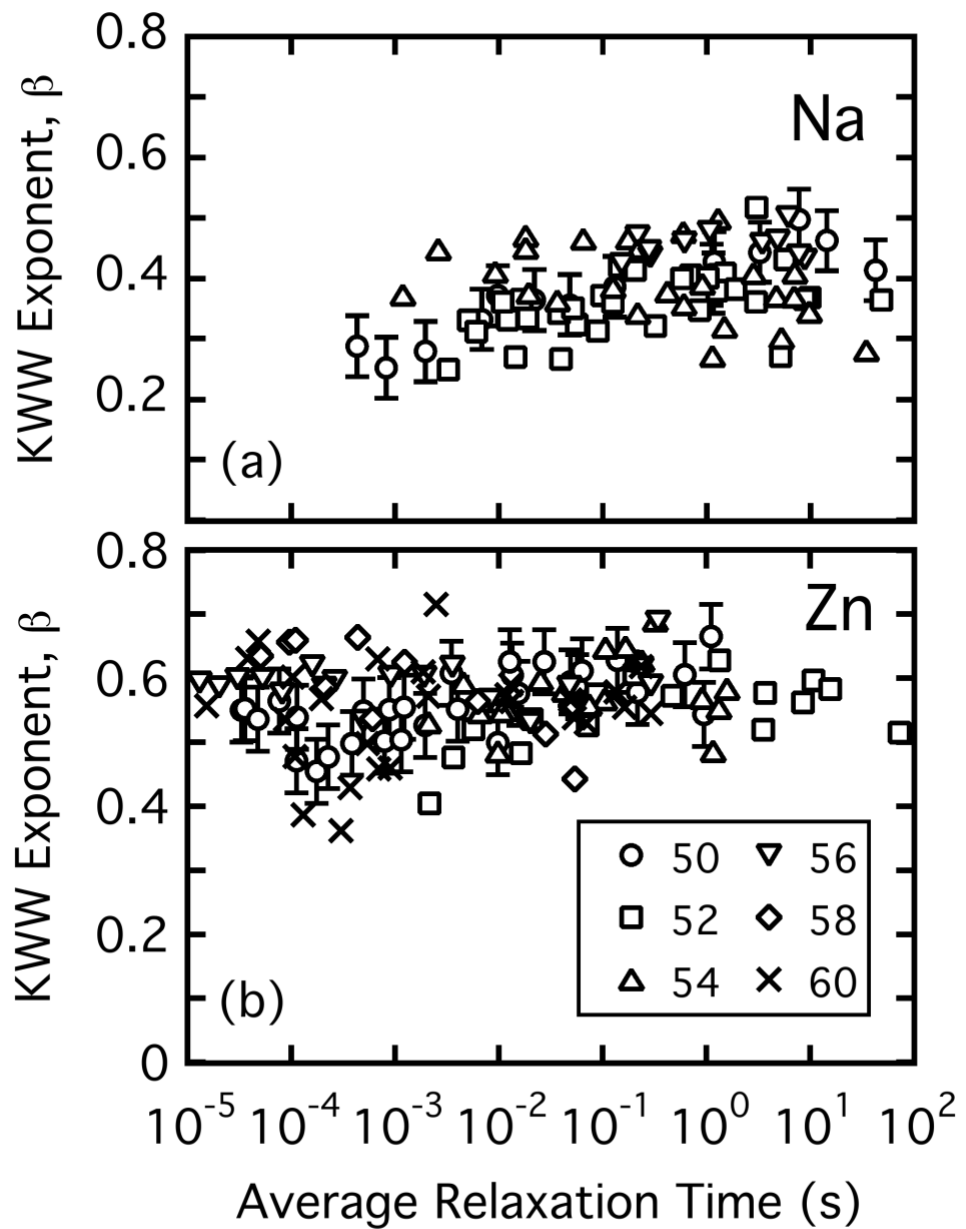


Fig. 5 The non-exponentiality exponent plotted against the average relaxation time for (a) sodium phosphate and (b) zinc phosphate melts. Symbols conform to a common key in the lower figure.